Supporting information

Deposition of MnO_2 on KOH-activated laser-produced graphene for a flexible planar micro-supercapacitor

XI Shuang[1,*], GAO Xing-wei[1], CHENG Xi-ming[1], LIU Hui-long[2,*]

（*1. College of Mechanical and Electronic Engineering, Nanjing Forestry University, Nanjing 210037, China;*
2. State Key Laboratory of Precision Electronic Manufacturing Technology and Equipment & School of Electromechanical Engineering, Guangdong University of Technology, Guangzhou 510006, China）

Corresponding author： XI Shuang, Associate professor. E-mail: shuangxi@njfu.edu.cn;
LIU Hui-long, Associate professor. E-mail: huilong.liu@gdut.edu.cn

The equation for evaluating the electrochemical performance of supercapacitors. The area specific capacitance $C_{A, GCD}$, was calculated using Equation (1) based on the constant current charge and discharge curves:

$$C_{A,GCD} = \frac{I\Delta t}{A\Delta V} \quad (1)$$

where $C_{A, GCD}$ is the area-specific capacitance, I is the current, Δt is the discharge time, A is the effective area of the electrode, and ΔV is the potential window after excluding the IR drop.

The area energy density E_A and area power density P_A are calculated using Equations (2) and (3), respectively:

$$E_A = \frac{1}{2} \times C_{A,GCD} \times \frac{(\Delta V)^2}{3600} \quad (2)$$

$$P_A = \frac{E_A \times 3600}{\Delta t} \quad (3)$$

where $C_{A, GCD}$ are area specific capacitances at different current densities, ΔV is the potential window after IR drop is excluded, and Δt is the discharge time.

Coulombic efficiency is calculated from 5000 charge/discharge cycles recorded at a current density of 0.2mA/cm^2 using equation（4）:

$$\eta = \frac{T_d}{T_c} \times 100\% \quad (4)$$

where η, T_d and T_c represent Coulomb efficiency, discharge time and charge time.

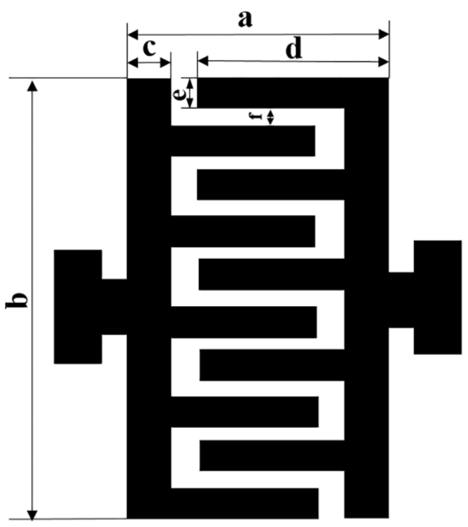

Figure S1. Geometry of electrodes with inserted finger structure

Table S1. Dimensional parameters of electrodes with finger insert structure（except for the two sides for easy clamping of the lugs）

Location	Dimension (mm)
Overall dimensions（a×b）	13.6×20.4
Width of the pad（c）	2.5
Finger electrode length（d）	10.5
Finger electrode width（e）	1.5
Vertical Gap between finger electrodes（f）	0.6

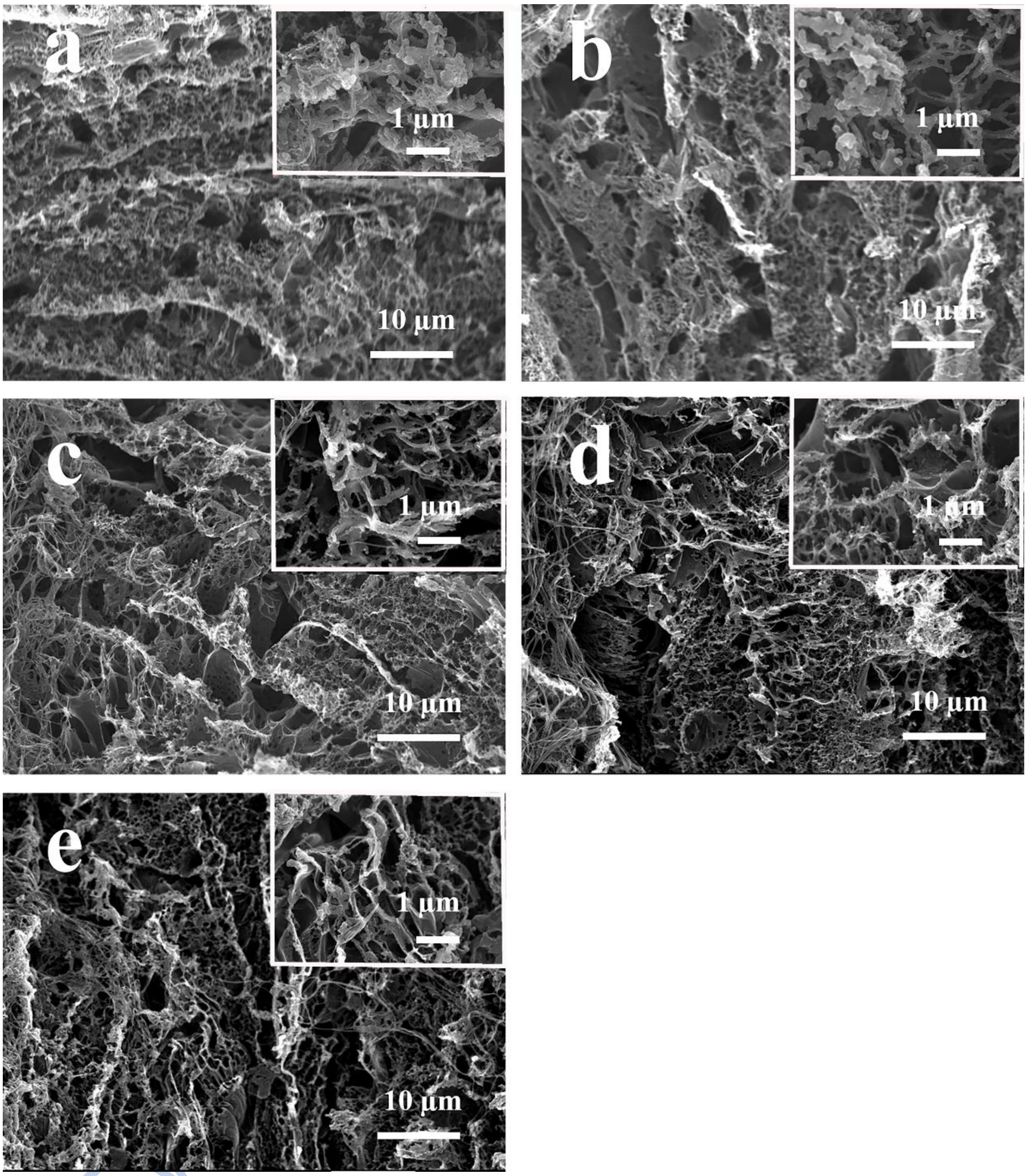

Figure S2. SEM images of (a) LIG, (b) a-LIG -280, (c) a-LIG -400, (d) a-LIG -560 and (e) a-LIG -1120.

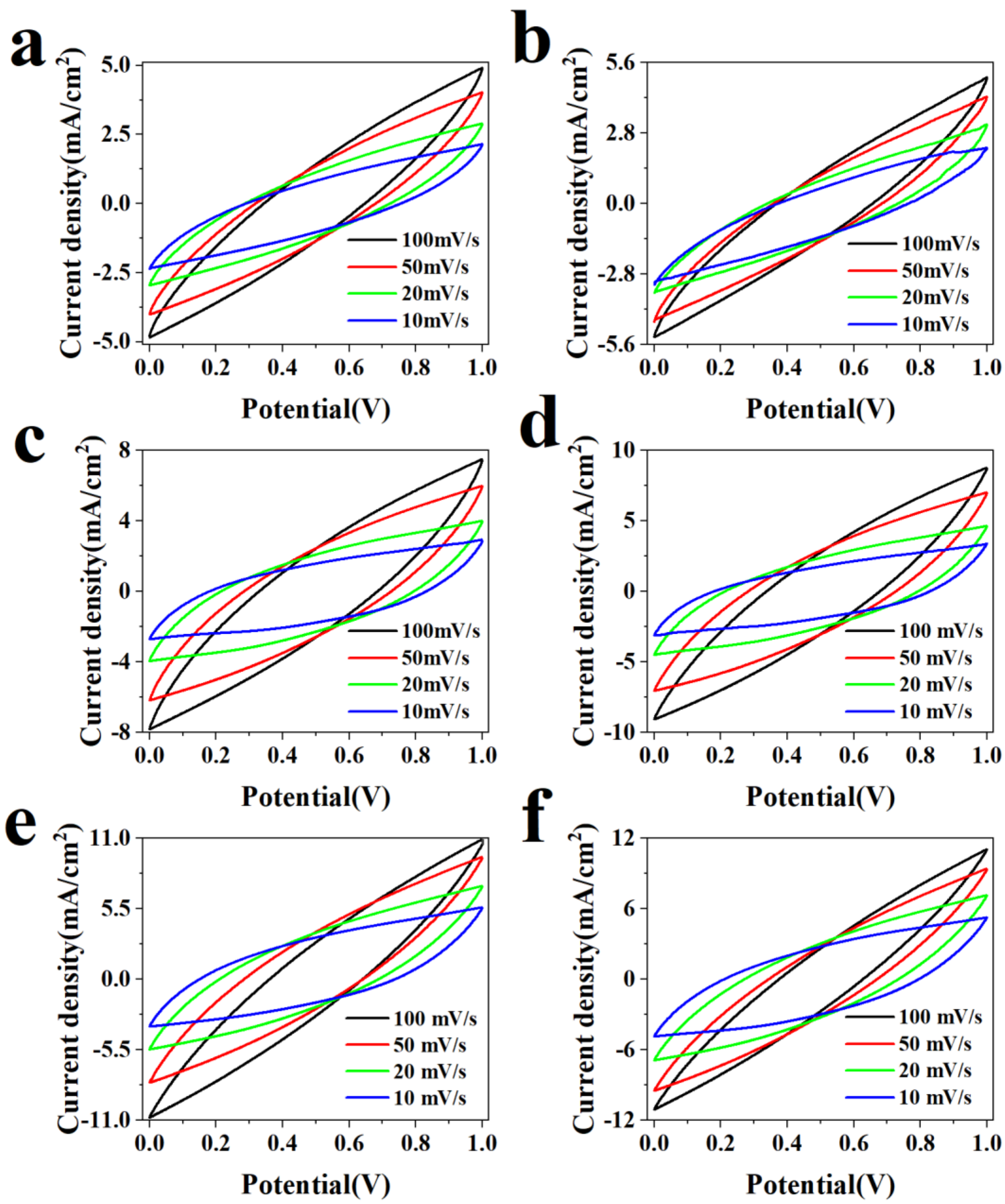

Figure S3. (a) Cyclic voltammetry curves of LIG, (b) a-LIG-0/ MnO_2, (c) a-LIG-280/MnO_2, (d) a-LIG-400/MnO_2, (e) a-LIG-560/MnO_2 and (f) a-LIG-1120/MnO_2 in a potential window from 0 to 1.0 V with scan rates ranging from 10 to 100 mV/s.

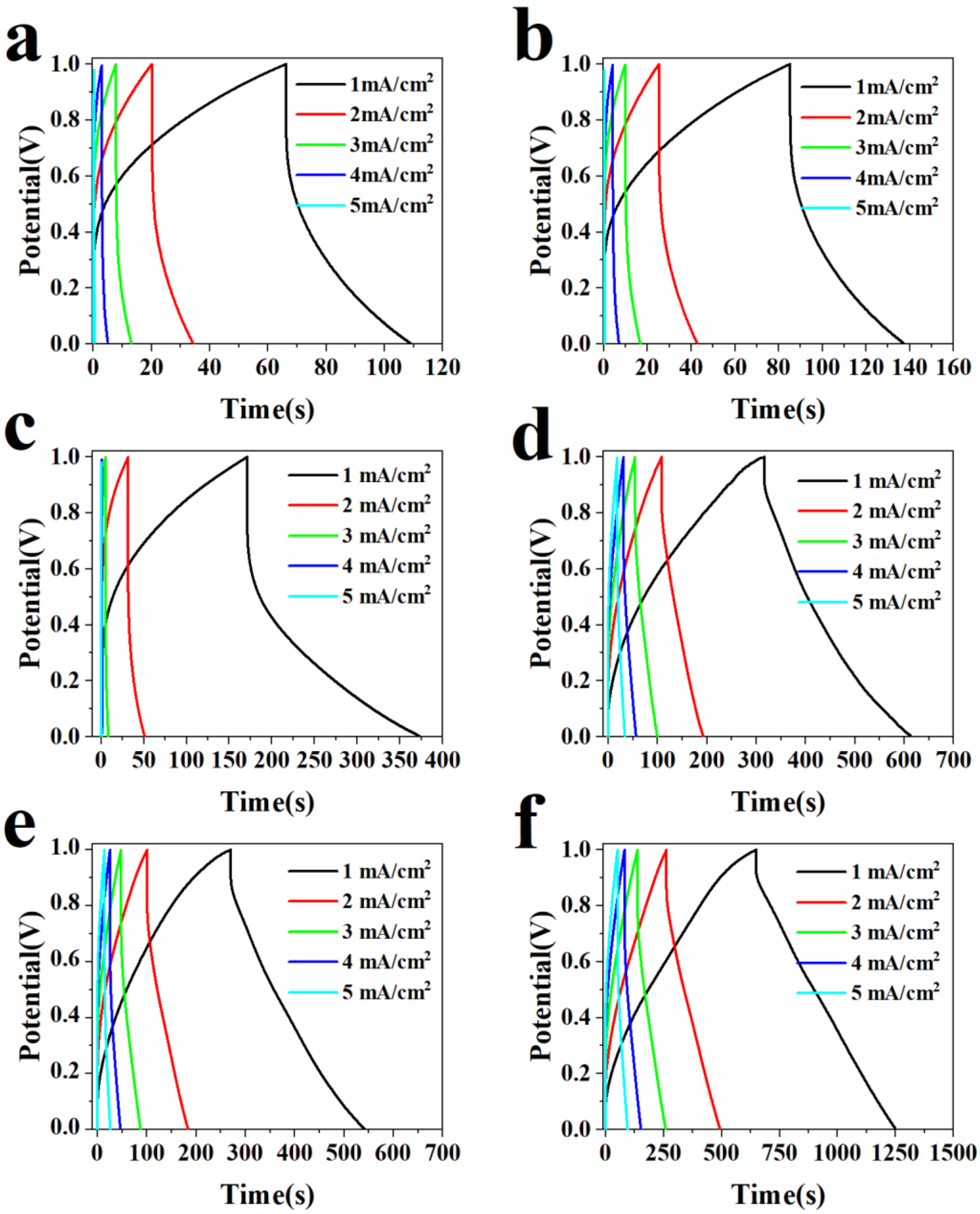

Figure S4. (a) Constant current charge/discharge curves for LIG, (b) a-LIG-0/MnO_2, (c) a-LIG-280/MnO_2, (d) a-LIG-400/MnO_2, (e) a-LIG-560/MnO_2 and (f) a-LIG-1120/MnO_2 in the potential window from 0 to 1.0 V for a current density range of 1 to 5 mA/cm^2.

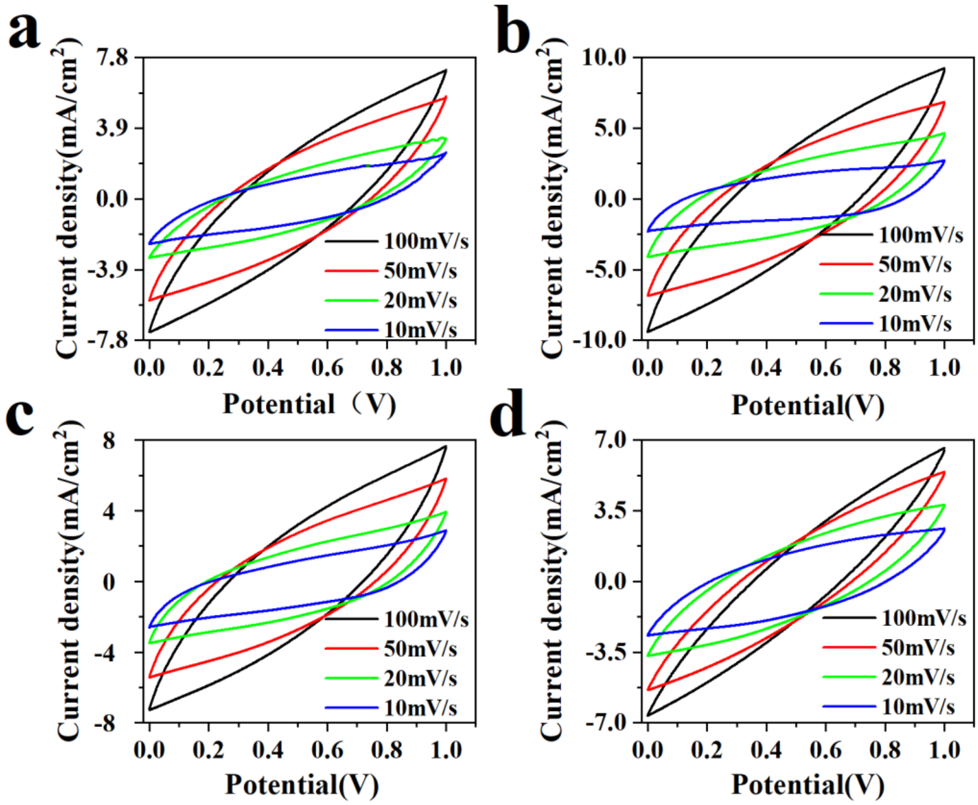

Figure S5. Cyclic voltammetry curves of (a) a-LIG/MnO_2-150s, (b) a-LIG/MnO_2-300s, (c) a-LIG/MnO_2-600s and (d) a-LIG/MnO_2-1000s in a potential window from 0 to 1.0 V with scan rates ranging from 10 to 100 mV/s.

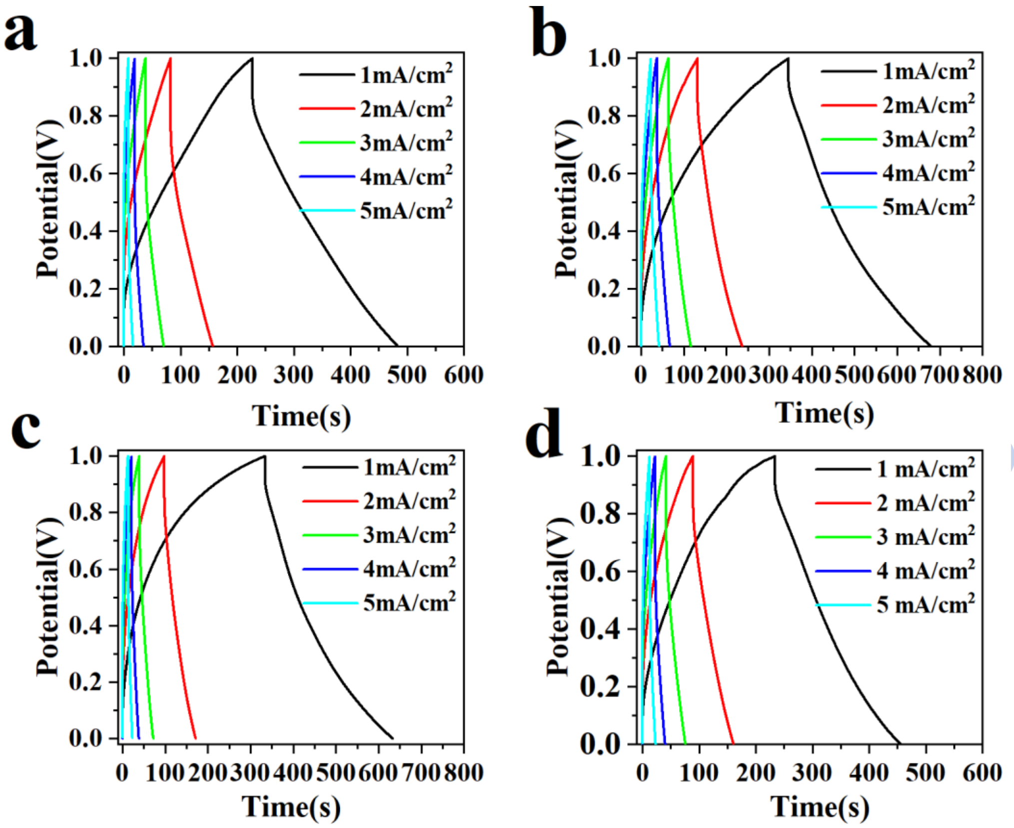

Figure S6. (a) Constant current charge/discharge curves for a-LIG/MnO_2-150s, (b) a-LIG/MnO_2-300s, (c) a-LIG/MnO_2-600s and (d) a-LIG/MnO_2-1000s in a potential window from 0 to 1.0 V for a current density range of 1 to 5 mA/cm^2.

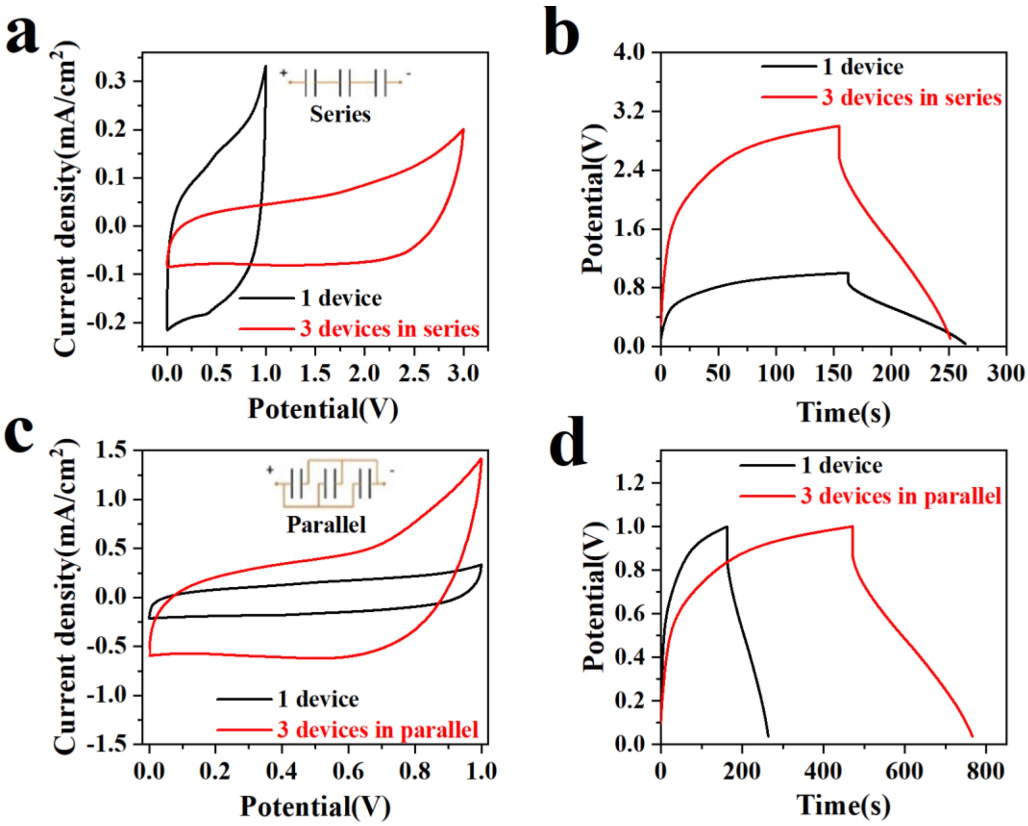

Figure S7. Assembly of multiple devices in parallel and series configurations. (a) Single-stage and series CV curves of a-LIG/MnO_2 @a-LIG at 10 mV/s scan rate. (b) Single-stage and series GCD curves of a-LIG/MnO_2 @a-LIG at a scan rate of 0.1 mA/cm^2. (c) Single-stage and parallel CV curves of a-LIG/MnO_2 @a-LIG at a scan rate of 10 mV/s. (d) Single-stage and parallel GCD curves of a-LIG/MnO_2 @a-LIG at 0.1 mA/cm^2 scan rate.

Table S2. Comparison of electrochemical performances for various laser-processed IMSC devices

Material	Electrolyte	Areal capacitance (mF/cm^2)	Energy density (μWh/cm^2)	Ref.
a-LIG/MnO_2 @a-LIG	PVA/H_3PO_4	18.82 at 0.2 mA/cm^2	2.61	This work
LIG	PVA/H_3PO_4	5.00 at 0.05 mA/cm^2	0.64	[1]
LIG	1 M H_2SO_4	4.00 at 20 mV/s	0.51	[2]
LIG	PVA/H_2SO_4	9.00 at 0.02 mA/cm^2	1.13	[3]
Fs-LIG	PVA/H_3PO_4	0.80 at 10 mV/s	0.07	[4]
B-doped LIG	PVA/H_2SO_4	16.50 at 0.05 mA/cm^2	2.11	[5]
MoS_2-LIG	PVA	14.00 at 10 mV/s	1.82	[6]
N-doped LIG with PEDOT	PAAK/KOH	0.79 at 0.05 mA/cm^2	0.06	[7]
MnO_2//Fe_2O_3	1 M KOH	8.39 at 20 mV/s	1.68	[8]
rG/SPANI//rG	PVA/H_2SO_4	3.31 at 10 mV/s	0.30	[9]
MnO_2/PPy// V_2O_5-PANI	PVA/LiC	~7.33 at 0.05 mA/cm^2	~2.45	[10]

References

[1] Liu H, Xie Y, Liu J, et al. Laser-induced and KOH-activated 3D graphene: a flexible activated electrode fabricated via direct laser writing for in-plane micro-supercapacitors[J]. Chemical Engineering Journal, 2020, 393: 124672.

[2] Lin J, Peng Z, Liu Y, et al. Laser-induced porous graphene films from commercial polymers[J]. Nature communications, 2014, 5(1): 5714.

[3] Peng Z, Lin J, Ye R, et al. Flexible and stackable laser-induced graphene supercapacitors[J]. ACS applied materials & interfaces, 2015, 7(5): 3414-3419.

[4] Jung B In, Ben H, Jae-Hyuck Y, et al. Facile fabrication of flexible all solid-state micro-supercapacitor by direct laser writing of porous carbon in polyimide. Carbon, 2015, 83, 144-151.

[5] In J B, Hsia B, Yoo J H, et al. Facile fabrication of flexible all solid-state micro-supercapacitor by direct laser writing of porous carbon in polyimide[J]. Carbon, 2015, 83: 144-151.

[6] Clerici F, Fontana M, Bianco S, et al. In situ MoS_2 decoration of laser-induced graphene as flexible supercapacitor electrodes[J]. ACS applied materials & interfaces, 2016, 8(16): 10459-10465.

[7] Song W, Zhu J, Gan B, et al. Flexible, stretchable, and transparent planar microsupercapacitors based on 3D porous laser-induced graphene[J]. Small, 2018, 14(1): 1702249.

[8] Liu Z, Tian X, Xu X, et al. Capacitance and voltage matching between MnO_2 nanoflake cathode and $Fe_2 O_3$ nanoparticle anode for high-performance asymmetric micro-supercapacitors[J]. Nano Research, 2017, 10: 2471-2481.

[9] Song B, Li L, Lin Z, et al. Water-dispersible graphene/polyaniline composites for flexible micro-supercapacitors with high energy densities[J]. Nano Energy, 2015, 16: 470-478.

[10] Yue Y, Yang Z, Liu N, et al. A flexible integrated system containing a microsupercapacitor, a photodetector, and a wireless charging coil[J]. Acs Nano, 2016, 10(12): 11249-11257.